Structural Engineering and Mechanics, *Vol. 64, No. 5 (2017) 543-555*
DOI: https://doi.org/10.12989/sem.2017.64.5.543

Studies on two bay and three storey infilled frame with different interface materials: Experimental and finite element studies

S. Muthukumar*[1], K.S. Satyanarayanan[1a] and K. Senthil[2b]

[1]*Department of Civil Engineering, SRM University, Kattankulathur, 603203, Tamil Nadu, India*
[2]*Department of Civil Engineering, NIT Jalandhar, Jalandhar, 144011, Punjab, India*

(Received April 14, 2017, Revised July 7, 2017, Accepted July 10, 2017)

Abstract. The non-linear behaviour of integral infilled frames (in which the infill and the frame are bonded together with help of various interface materials) is studied both experimentally and numerically. The experiments were carried out on one-sixth scale two-bay and three-storey reinforced concrete frames with and without infill against static cyclic loading. Three interface materials - cement mortar, cork and foam have been used in between the infill and the frame. The infill, interface and the frame are bonded together is called integral frame. The linear and non-linear behaviors of two dimensional bare frame and integral infilled frame have been studied numerically using the commercial finite element software SAP 2000. Linear finite element analysis has been carried out to quantify the effect of various interface materials on the infilled frames with various combinations of 21 cases and the results compared. The modified configuration that used all three interface materials offered better resistance above others. Therefore, the experiments were limited to this modified infilled frame case configuration, in addition to conventional (A1-integral infilled frame with cement mortar as interface) and bare frame (A0-No infill). The results have been compared with the numerical results done initially. It is found that stiffness of bare frame increased by infilling and the strength of modified frame increased by 20% compare to bare frame. The ductility ratio of modified infilled frame was 42% more than that of the conventional infilled frame. In general, the numerical result was found to be in good agreement with experimental results for initial crack load, ultimate load and deformed pattern of infill.

Keywords: infilled frame; cement mortar; cork; foam; cyclic loading; earthquake engineering; finite element analysis

1. Introduction

The reinforced concrete frames with masonry infill walls are widely used in buildings. In urban areas, 30% buildings were reinforced concrete moment resisting frame, 48% were brick masonry and 22% were rubble masonry. In rural areas, 82% of buildings were brick masonry while 18% were reinforced concrete frame. Therefore, the safety of the masonry building is very important in the moderate to severe seismic zones, as 90% of the world population lives and works in masonry buildings and these buildings should be protected during earthquakes, Erdik and Aydinoglu (2003). The post-earthquake reconnaissance surveys showed by Dogangun *et al*. (2008), the lack of lateral strength together with masonry infill, frame element and interface element for collapse in most cases. Failures of both reinforced and unreinforced masonry in-plane is so common that it is almost taken for granted and forgotten, Key (1988). In-plane masonry is very stiff, so that the forces transmitted by ground shaking are high, and brittle so that failure is accompanied by a marked reduction in strength and stiffness. Although the infill panels significantly enhance both the stiffness and strength of the frame, their contribution is often not considered mainly because of the lack of knowledge of the composite behaviour of the frame and the infill. However, extensive experimental (Smith 1967, Mehrabi *et al*. 1996), semi analytical investigations (Liauw and Kwan 1984, Dhanasekar and Page 1986, Asteris 2003, Moghaddam 2004) and numerical investigations (Mallick and severn 1967, Mallick and Garg 1971, Ibrahimbegovic 1990, Ghosh and Amde 2002, Khoshnoud and Marsono 2016) has been carried out in last six decades. Mehrabi *et al*. (1996) have carried out experimental and analytical studies on masonry-infilled reinforced concrete frames under in-plane lateral loadings. A smeared-crack finite element model was used to model the behavior of concrete in the RC frames and masonry units. Authors concluded that the finite element models are able to simulate the failure mechanisms exhibited by infilled frames including the crushing and cracking of the concrete frames and masonry panels and the sliding and separation of the mortar joints.

Liauw and Kwan (1984) conducted experimental and numerical investigations on one-bay four-storey non-integral infilled frames to study the non-linear behaviour. It is concluded that the strength of non-integral infilled frames is highly dependent on the bending strength of the frame. Dhanasekar and Page (1986) carried out finite element analysis to simulate the behaviour of infilled frame subjected to racking loads. It is concluded that the behaviour of the composite frame influenced by the strength properties of the masonry such as the magnitude of the

*Corresponding author, Research Scholar
E-mail: sevens.muthu@gmail.com
[a]Professor
[b]Assistant Professor

ISSN: 1225-4568 (Print), 1598-6217 (Online)

shear and tensile bond strengths relative to the compressive strength. Mallick and Severn (1967), Mallick and Garg (1971) suggested first finite element approach to analyse infilled frames, addressing the problem of an appropriate representation of the interface conditions between frame and infill. Several single story rectangular infilled frames under static loading were analyzed and the results were in a good agreement with experimental results if the height to span ratio was not greater than two. The finite element model by Ghosh and Amde (2002) includes interface elements in between frame and masonry infill. They predicted the failure mode and the minimum principal stress on infill flexible frame against 216 kN lateral load and the infill stress is very high at the corners, 11,600 kN/m^2 and similar results were predicted numerically by Senthil (2010), Senthil and Satyanarayanan (2016), and the stress at the corners is 1500 kN/m^2 against lateral load of 60 kN. Khoshnoud and Marsono (2016) developed a simple method, called corner opening, by replacing the corner of infill walls with a very flexible material to enhance the structural behavior of walls. In addition to that few experimental and numerical studies including authors previous work was found on masonry infilled reinforced concrete with various interface materials, different type of infill under seismic loadings, (Klingner and Bertero 1978, Riddington 1984, Buonopane and White 1999, Al-Chaar *et al.* 2002, Anil and Altin 2007, Satyanarayanan 2009, Satyanarayanan and Lakshmipathy 2009, Senthil *et al.* 2016a, b) and based on the finite element modelling by (Muthukumar *et al.* 2017). Based on the literature survey, it is observed that most of the weakest spot of the building are reinforced concrete frame element and infill masonry wall element which in spite of bonding layers of interface element.

The review of literature carried out has indicated that study on effect of interface of frame and infill as well as influence of various interface materials is limited. In practice the load transferring beam-column frame system is filled in with masonry for functional purpose. These walls are jointed to the soffit of beam and column without leaving a gap in between them by cement mortar. The aim of filling up the gap is mainly to improve the privacy through sound insulation and also helps in thermal insulation. In modern times, cork/foam materials are used for the purpose instead of cement mortar. According to the authors, the influence of various interface materials on the infilled frames has not been studied. In the present study, experimental and numerical investigations were carried out to quantify the effect of interface on the behaviour of infilled frames with respect to lateral stiffness, initial and ultimate load. The experiments were carried on one-sixth scale two-bay and three-storey reinforced concrete frame with and without infill against static cyclic loading. The details of the frame are given in section 2.1. The three different interface materials such as cement mortar, cork and rubber foam has been used in between the infill and the frame are bonded together is called integral frame. The interface materials of 5 mm thickness were used around inside the reinforced concrete frame. The behavior of bare frame and integral infilled frame has been studied numerically using

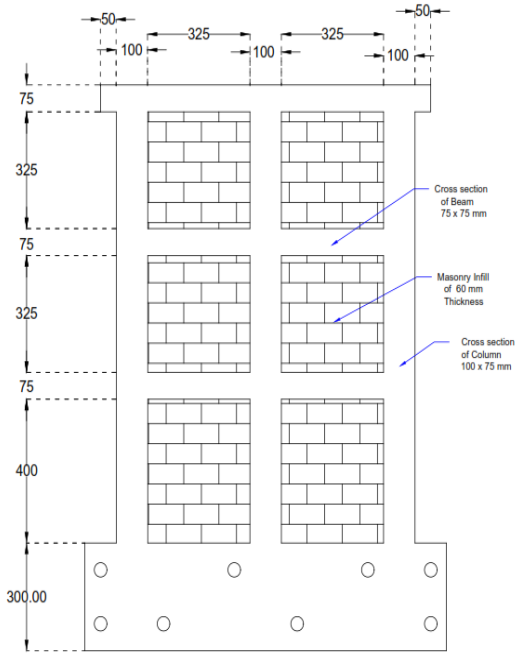

Fig. 1 Schematic of infilled frame

commercial finite element software SAP 2000. The response of integral infilled frame with various interface materials in combinations (A0, A1, A2….. A21) of configuration at storey level has been studied numerically and compared.

2. Materials and modeling

The numerical investigation was carried out on two-bay three storey integral infilled frame as well as bare frame using SAP 2000 Version 14. The behaviour of bare frame as well as integral infilled frame has been studied using linear finite element analysis. In this Section, the preliminary investigations on reinforced concrete frame, testing on materials and methodology for finite element analysis has been presented and discussed. Linear finite element analysis has been carried out to quantify the effect of various interface materials on the infilled frames and discussed in Section 3. In Section 4, the experiments were carried out on bare frame as well as selected integral infilled frame based on the linear analysis in Section 3 and discussed. The non-linear finite element analysis has been carried out to estimate the strength capacity of a structure beyond its elastic limit to its ultimate strength and discussed on Section 5. The results obtained through numerical simulations in terms of first crack load, ultimate load, location of plastic hinges and stress on infill has been compared with the experiments also discussed in Section 5.

2.1 Preliminary studies

The detailed dimensions of concrete frame and reinforcement bar has been shown in Figs. 1 and 2 respectively. The finite element model has been developed

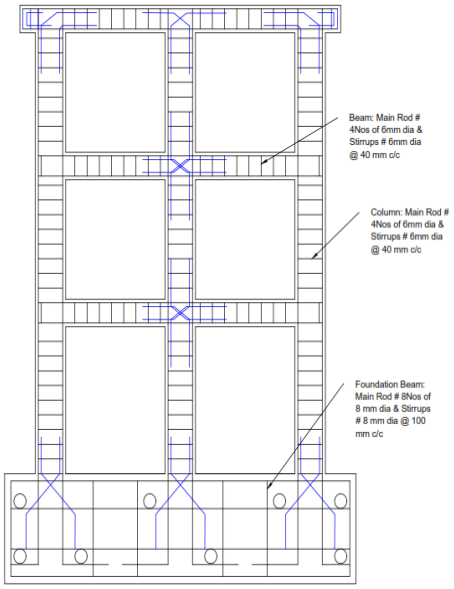

Fig. 2 Schematic of reinforced bar details

is a scaled model, actual building scaled to a factor of 1:6. The size of beam and column is 75×75 mm and 100×75 mm were considered. Base beam of length, width and depth are 1200, 250 and 300 mm respectively has been used in the present study considering the point of stability of frame during application of loading, see Fig. 1. The main reinforcement of 4 numbers of 6 mm diameter and 6 mm stirrups at 40 mm spacing was considered. For base beam, the detailed schematics of reinforcements used is shown in Fig. 2. The size of infill panel was 325×400 mm at ground floor panel whereas 325×325 mm first and second floor, and the masonry infill of 60 mm thickness has been used.

2.2 Material testing

The material tests on concrete, masonry, cement mortar, cork and foam has been carried out in the laboratory as per the procedure recommended by Indian Standard. The plain concrete cube having a Mix 20 designed and characteristic compressive strength of 28.5 MPa was obtained through cube compressive strength of 28 days curing and their properties are shown in Table 1. For concrete, the modulus of elasticity is taken as that recommended by IS 456:2000, that is $5000\sqrt{f_{ck}}$ MPa where f_{ck}characteristic compressive strength of 28.5 MPa. The reinforced bar of f_y 415 grade steel having characteristic strength of 415 MPa has been used and their Young's modulus has been chosen as 200000 MPa. Poisson's ratio of concrete and steel was taken as 0.2 and 0.3 respectively commonly adopted for the design. The compressive strength of second class brick masonry prism at 28 days is 4.55 MPa was obtained from the experiments and their flexural tensile strength, Young's modulus and Poisson's ratio is 0.3 Mpa, 3018.2 Mpa and 0.22 respectively. The cube compressive strength of 1:5 (Cement:Sand) cement mortar 2.78 MPa was obtained from the experiments and, the modulus of elasticity and Poisson's ratio has also been obtained as 1167 MPa and 0.15, respectively. Similarly, the elastic properties of

Table 1 Properties of reinforcing bar, concrete, infill and interface material

Description	Young's Modulus (MPa)	Compressive strength (MPa)	Poisson's ratio	Density (kN/m^3)
Reinforcement	200000	-	0.3	76.9
Concrete	26706	28.53	0.2	24.9
Infill (Brick Masonry)	3018.2	4.55	0.22	13.2
Interface (Cement mortar)	1167	2.78	0.15	18.0
Interface (Cork)	12.6	-	0.097	1.7
Interface (Foam)	2	-	0.49	0.24

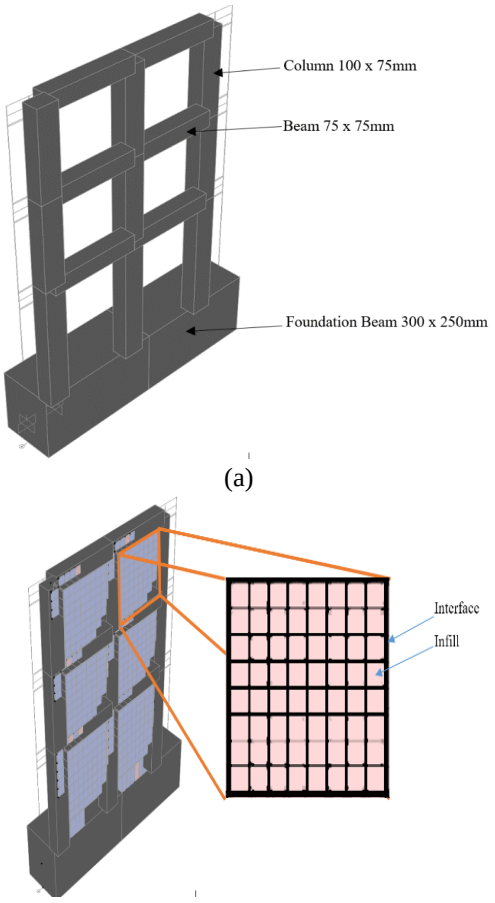

Fig. 5 Finite element mode of typical (a) bare frame and (b) infilled frame

interface materials such as cork and foam has also been studied. The cork sheet of type A and black flexible polymer foam were procured in the form of sheet of 5 mm thickness.

2.3 Finite element modelling of bare frame and integral infilled frame

The frame members were modelled as beam and column line elements, while the infill and interface elements were modelled as shell elements with plane sections, see Fig. 5. The mesh convergence study has been carried out on infill by varying the element size from 1×1, up to 16×16. The

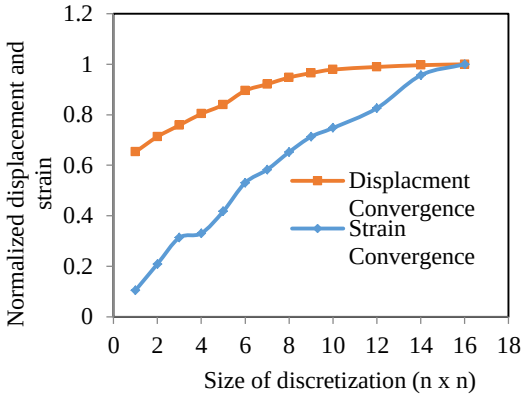

Fig. 6 Mesh convergence study

infill and interface elements were shell elements and discretized as area mesh. The mesh sensitivity was studied in terms of displacement of frame and strain in infill. The monotonic convergence is found with reference to displacements. However the strain value did not show such a pattern. Hence only the displacement has been considered for mesh sensitivity studies. The displacement of the frame was found to increase up to a mesh size of 8×8 as shown in, Fig. 6.

Therefore a discretization of 8×8 elements was adopted in the analytical work throughout. The interface elements are discretised as 8×1 at top and bottom of the infill and 1×8 at left and right side of the infill. The node element model has been used to discretize the beam and column element whereas finite element model is used for infill and interface. The beam and column elements are discretized as 1×8, auto meshing at intermediate points was specified and generated according to mesh size on infill. Node element model in structural elements are represented by individual lines connected by nodes. A node element model is technically a finite-element model in which a single line element represents the structural element, (SAP 2000). Node element modelling, however, follows the direct stiffness method, whereas finite element modelling follows the finite element method. Finite element model with a meshing procedure creates a network of line elements connected by nodes within a material continuum.

The boundary conditions were assigned as a fixed joint and zero displacement was specified for fixed degree of freedom at restraint support locations. The fixed restraints were assigned at foundation level of beam column joints. A link element was used to connect two joints, separated by thickness or width of interface, such that specialized structural behaviour was modelled. The linear properties were assigned to link elements such that directional properties of U1, U3 and R2 are restrained. Based on the developed forces in these linkage elements, separation between infill and frame was assumed to occur. The connection of link elements and masonry infill, interface elements are enabled to take tension and shear forces, the interaction between the frame and the infill through this mortar joint is modeled by an interface element capable of transferring normal and shear forces in the elastic and inelastic ranges of loading. All the finite element models

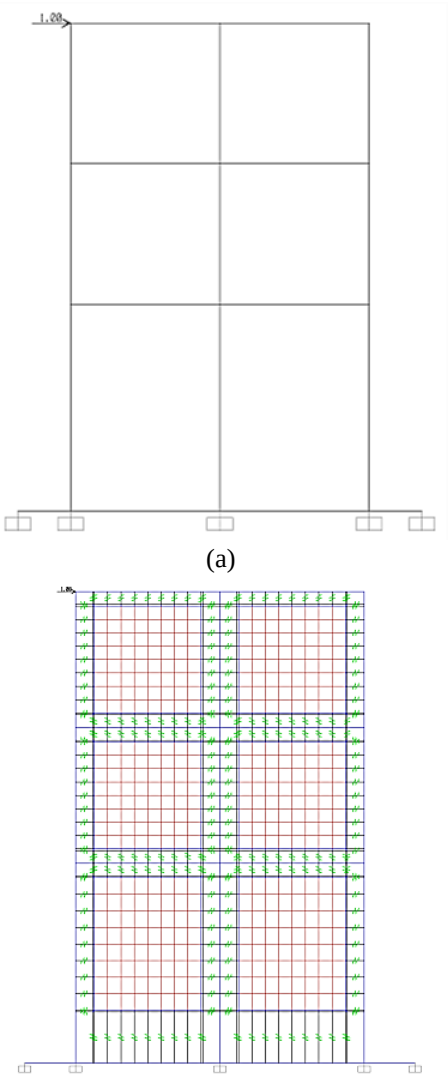

(a)

(b)

Fig. 7 Application of loading on typical (a) bare frame and (b) infilled frame

were analyzed by applying lateral load alone. The frames were loaded at storey level at the top left corner with 1 kN lateral forces (typical loading) as point load, see Fig. 7(a)-(b). The response of the infilled frame as well as bare frame in terms of deflections was measured at the top right corner. The interface materials of 5 mm thickness was used around inside the reinforced concrete frame.

3. Selection of interface material combination through linear finite element analysis

Finite element models that have been developed to quantify the effect of various interface materials on the infilled frames are proposed to carry out linear numerical investigation as outlined in this Section. Twenty one different sets of interface materials were employed in the present study to investigate the response of infilled frame against lateral load, Table 2. The objective behind choosing the twenty one different sets of interface materials was

Table 2 Details of interface materials at different storey level

Description	Ground floor	First floor	Second floor
A0	Bare frame (No infill and interface)		
A1	M	M	M
A2	F	F	F
A3	C	C	C
A4	M	M	F
A5	M	M	C
A6	F	F	M
A7	F	F	C
A8	C	C	M
A9	C	C	F
A10	M	F	F
A11	C	F	F
A12	F	C	C
A13	M	C	C
A14	C	M	M
A15	F	M	M
A16	C	F	M
A17	F	C	M
A18	C	M	F
A19	M	C	F
A20	M	F	C
A21	F	M	C

Table 3 Comparison of stiffness of infilled frame using linear finite element analysis

Interface configuration	Initial stiffness kN/mm	% of drop in stiffness compare to A1
A1	28.24	0.0
A2	7.824	72.3
A3	8.396	70.3
A4	18.587	34.2
A5	19.083	32.4
A6	10.266	63.7
A7	7.974	71.8
A8	10.845	61.6
A9	8.237	70.8
A10	12.15	57.0
A11	8.051	71.5
A12	8.163	71.1
A13	12.789	54.7
A14	15.128	46.4
A15	14.598	48.3
A16	12.484	55.8
A17	10.471	62.9
A18	11.848	58.1
A19	12.437	56.0
A20	10.537	62.7
A21	11.709	58.5

obtaining better correspondence for predicted responses of infilled frame against the infilled frame with various configuration. The interface material was recognized as cement mortar (M), cork (C) and foam (F) and their effect was studied by placing at ground, first and second floor level. The lateral load considered in the present study was arbitrary. All the models were analyzed by applying lateral load. The chosen 21 configurations were loaded at top storey level at the top left corner with 1 kN lateral forces as nodal point load. The initial stiffness of the integral infill has been predicted and presented in the Table 3. The stiffness of conventional infilled frame A1 was found highest, i.e., 28.2 kN/mm, among 21 chosen configurations. Whereas the drop in stiffness of A2 configuration was found maximum as 72% i.e., 7.8 kN/mm. The stiffness of frame with A5 configuration was found to be decreased only 32% and this configuration consist of only cement mortar and cork. The overall drop in stiffness of integral infilled frame was found between 72-32% for the case in which various combination of interface materials (A2-A21) as compare to A1, see Table 3.

The simulations were carried out on A2-A15 configuration which consist of any two interface materials among cement mortar, cork and foam. The stiffness of some of these configuration was too low, i.e., A2, A3, A7, A9, A11 and A12, and for some cases it is too high, i.e., A4 and A5. Also, the simulations were carried out on A16-A21 configurations which consist of three interface materials at different storey level. The drop in stiffness of these configuration was found between 55-62% and it is observed that the performance of infilled frame with three interface

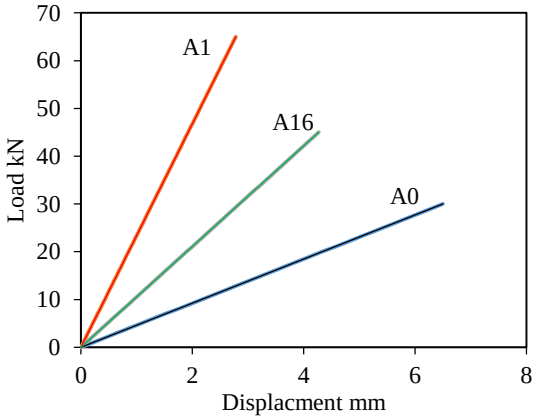

Fig. 8 Displacement of A0, A1 and A16 configuration function of loading

materials seems stable. The interface materials such as cork and foam are very soft as compared to cement mortar they may be considered equivalent to the presence of gap. The analysis considering the presence of gaps equivalent negligible elastic properties of interface materials lead to a stiffness of 5.6 kN/mm closer to the stiffness of bare frame. The load versus displacement curve of all 21 configurations has been predicted and shown for only A0, A1 and A16. However, it was observed that the displacement of A1 is almost 2 mm and corresponding load is 65 kN whereas other combination, for instance A16, the displacement is 4 mm against 45 kN, see Fig. 8. Therefore, it is concluded that the configuration A16 has been selected considering the ductility in terms of large displacement. The configuration

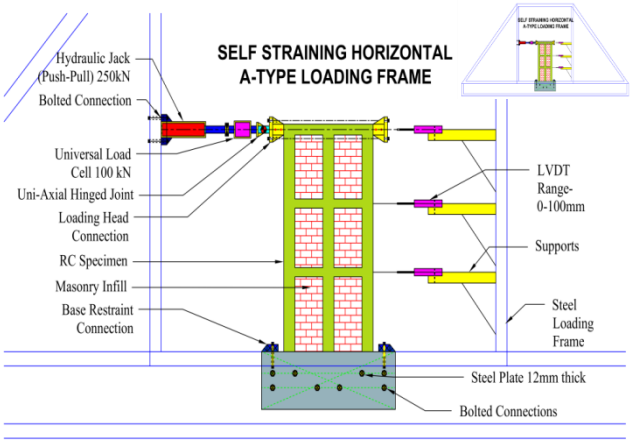

Fig. 9 Schematic of experimental setup

A16 describes infilled frame with cork as interface at ground storey, foam at first storey and cement mortar at second storey has been studied experimentally. Also the experiments were carried out on A1 and A0 configurations and compared with A16 and discussed in Section 4.

4. Experimental investigation

The experiments were carried out on two-bay three-storey bare frame (A0), integral infilled frame with cement mortar interface (A1) and various combination of interface (A16). The description of these models is given in Section 2.1 and the detailed schematics are presented in Figs. 1 and 2. The properties of plain concrete, infill and cement mortar was maintained remain same throughout the entire experimentation. The results obtained in terms of storey drift, hysteresis behaviour of frame, initial and ultimate load and ductility ratio were discussed in this section.

4.1 Preparation of specimens and experimental setup

The mould used for casting is arranged on a clean flat and non-absorbent surface. The reinforcement cage is placed inside the mould and cement mortar cover blocks. The exact quantities of materials are kept ready on another platform for preparing specimen and after mixing the concrete is filled as 3 layers in the mould. After that all the frames casted are covered with help of gunny bag and cured under sprinkling of water at regular interval for 28 days. The brick work has been done using solid cut bricks of uniform size. Standard size of solid brick is 200×100×75 whereas solid cut brick units with a nominal dimension of 100×60×75 mm was used. To include the number of masonry joints in scaled wall as in prototype wall. The specimens A1 and A16 are infilled and kept for curing for 3 days. After that the specimens were plastered 10 mm thickness with 1:5 mix ratio and again the specimen has been cured for 28 days. The specimen A1 and A16 were used for testing almost after 60 days whereas the specimen A0 was tested after 28 days. The specimen was wiped off its surface moisture and grit on the previous day of its testing date and it is white washed. The self-straining

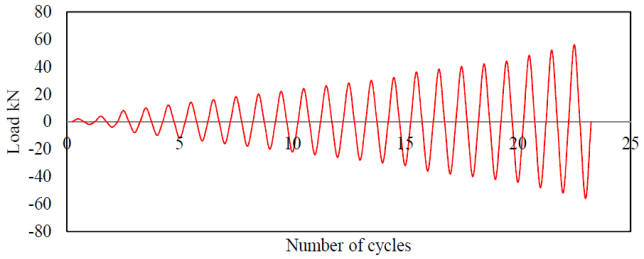

Fig. 10 In-plane loading profile for experiment

horizontal A-Type loading frame of 400 kN capacity platform is used for testing of specimens. The specimen is hauled to the Horizontal A-Type loading frame with the help of crane. The specimen is erected on the loading frame vertically and the frame is adjusted such that loading is in-plane, see Fig. 9. The displacement of frame was observed by using three LVDT's are placed at storey level. The LVDT (Linear Variable Differential Transformer) having push pull capacity of 100 mm connected to displacement indicators and it has been recorded. Hydraulic push pull jack which can be operated with a pumping unit of capacity 200 kN is attached with a universal load cell of capacity 100 kN which is connected to a load indicator. The load cell is connected to a hinge type end to effectively transfer the load instead of converting into moment to the specimen. The lateral load considered in the present study was arbitrary and it describes that the cyclic loading with 1 and 2 kN as increment achieved by each cycle for bare frame and infilled frame respectively, see Fig. 10.

4.2 Summary of experimental results

The behaviour of bare frame as well as infilled frame is discussed in terms of its hysteresis behaviour of frame, initial and ultimate load, storey drift and ductility ratio were discussed in this section. The initial cracking and ultimate load of specimens of A0, A1 and A16 specimens are presented in Table 4. The cyclic loading of the A0 frame has resulted in cracking of concrete at load level of 12.05 kN at joint of the frame. Initial cracks was found in the leeward (pull) side of the beam column joint of bare frame, see Fig. 11(a). On further loading the cracks increased in their length and width at the same sections. The failure of A0 frames was occurred at 33.15 kN. The critical hinge is formed at first and second storey at 32 kN in case of bare frame.

The cyclic loading of the A1 frame has resulted in cracking of concrete at load level of 30.03 kN at joint of the frame. Initial cracks was found to occur only at ground storey column along the Leeward (pull) side of loading. Also the interface bonding cracks was observed on ground storey right side panel at same initial cracking load, see Fig. 11(b). On further loading the cracks increased in their length and width at the same section and location. At 36 kN load, the cracks in small width in many numbers was observed in the windward ground storey column. On further loading, the crack in the masonry infill of ground storey right side panel was found increased significantly and similar pattern of cracks was observed on ground storey left

Table 4 Comparison of initial cracking and ultimate load of specimens

Configuration of frame	Initial cracking load kN	Ultimate load kN
A0	12.05	33.15
A1	30.03	60.04
A16	22.18	40.54

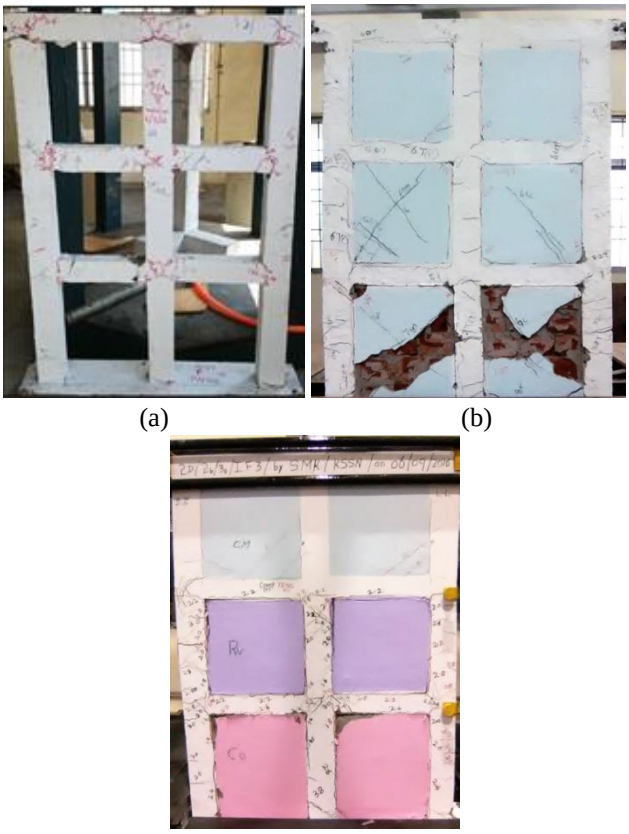

(a) (b)

(c)

Fig. 11 Deformed profile of (a) bare frame and infilled frame with (b) A1 and (c) A16 configuration

side panel. Further, the "*X*" crack was observed clearly in the masonry infill at first floor and seems the same trend was approaching at second floor. Damage normally comprises either collapse or diagonal cracking in both directions i.e., "*X*" cracking, Key (1988). It may be due to the fact that the stresses are transferred by the Infill by diaphragm action to the leeward side column equally transmitting the stresses without accumulating them in a particular point. The failure of A1 frames was occurred at 60 kN, almost twice to that of bare frame A0. It may be concluded that the infill panels (A1) significantly enhance both the stiffness and strength of the frame.

In case of infilled frame A16, initial crack occurs at 22.18 kN and the resistance at this level was found to be decreased 26% as compare to A1 frame. The first crack at top storey infill was observed against 30 kN, however the frame A16 lost their strength completely at 40 kN. It was also observed that the interface bonding crack at ground and first storeys at 16.4 kN, see Fig. 11(c). It is due to sliding shear failure through bed joint of a masonry infill associated

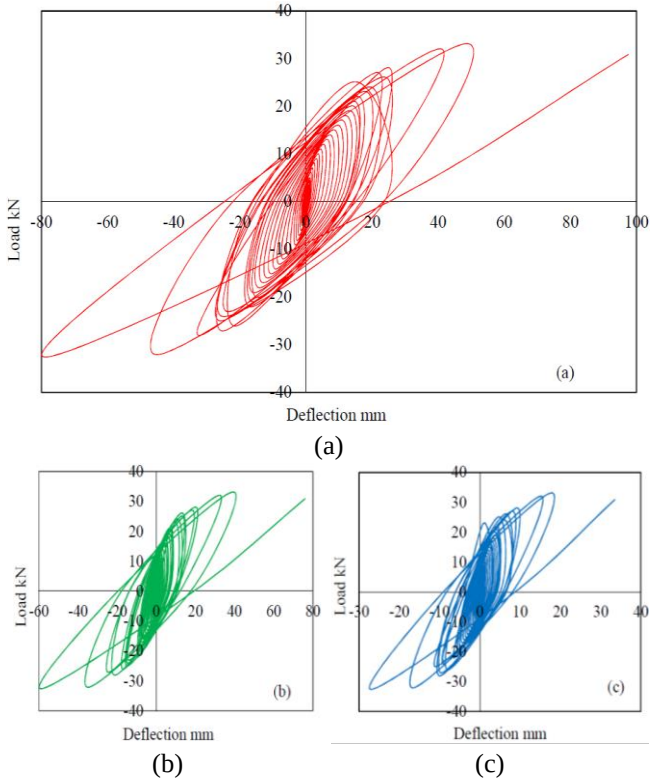

(a)

(b) (c)

Fig. 12 Hysteresis response of bare frame of (a) second (b) first and (b) ground storey

with infill with weak joints and strong members. The formation of shear crack separates the panel into two parts, which reduces the effective column height. Hence, the critical hinge was formed at ground and first storey of A16 frame, see Fig. 11(c). There is no diagonal crack was observed at ground and first storey of A16 infill but in case of A1 frame it appears at earlier stage. It may be due to the fact that the interface medium effectively transferring the lateral load from frame to infill. It is concluded that the influence of interface material (M) at second floor became rigid and first and ground floor having interface material (cork and foam) performing as a soft storey, but these storeys has internal stiffness.

The hysteresis response of A0 frame was measured at ground, first and second floor level against static cyclic loading is shown in Fig. 12(a)-(c). The frame A0 was able to support the cyclic loading upto 39 cycles but the frame A1 and A16 frame went only upto 24 and 21 cycles respectively. First crack was observed at 17th cycle against 12.05 kN. The amount of displacement in A0 frame was stable upto 31 cycles (15 mm) thereafter the displacement was found increased significantly, see Fig. 12(a). The displacement was found to be increased from 15 mm (31th cycle) to 24 mm (37th cycle) corresponding load 22 to 28 kN. The frame A0 almost lost their strength at 33 kN, however the displacement at 37th and 38th cycle was 40 and 48 mm with the increment of 1 kN respectively. Similarly, the displacement at first and ground floor at 26th cycle was 6 and 4 mm respectively, see Fig. 12(b)-(c). At failure, the displacement at second, first and ground floor was 98, 76

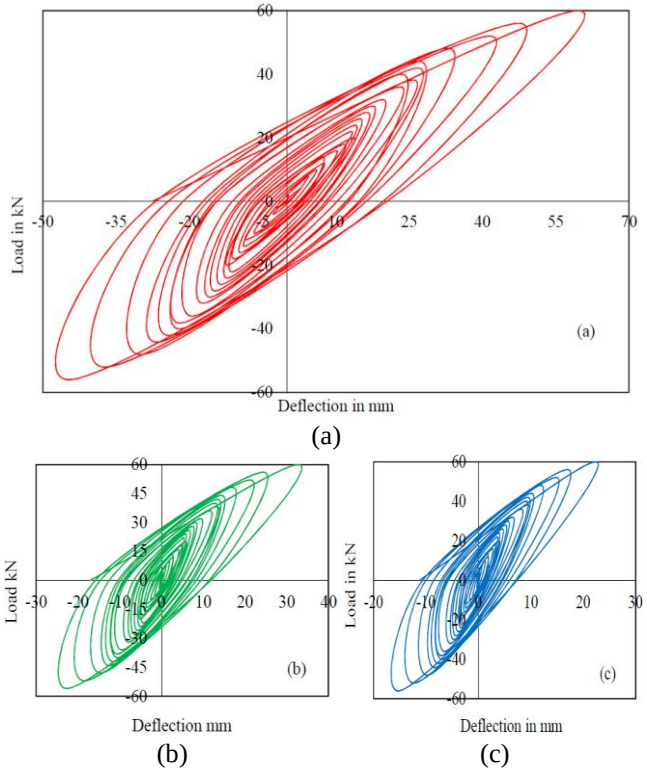

Fig. 13 Hysteresis response of A1 frame of (a) second (b) first and (c) ground storey

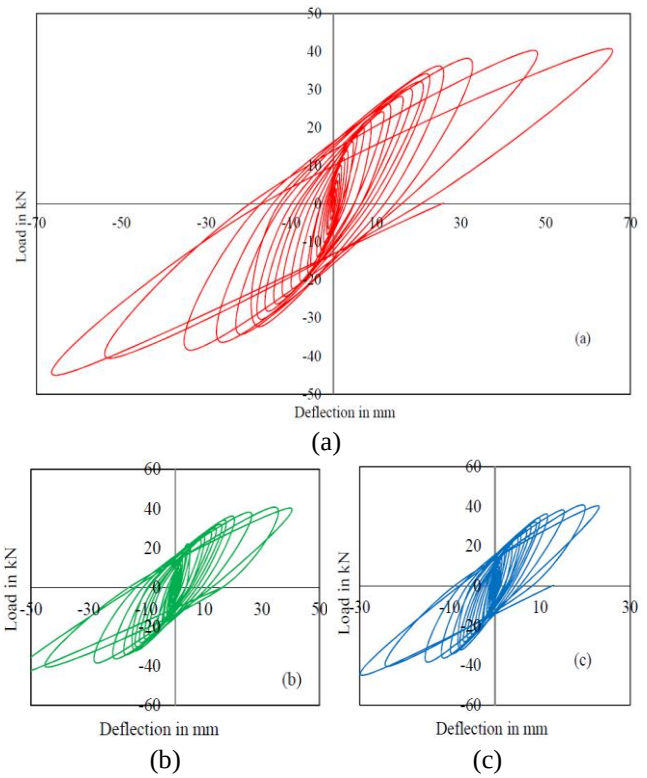

Fig. 14 Hysteresis response of A16 frame of (a) second (b) first and (c) ground storey

and 33 mm respectively.

The hysteresis response of A1 frame was measured at ground, first and second floor level against cyclic loading is shown in Fig. 13(a)-(c). First crack was observed as interface de-bonding at 7th cycle against 16 kN, however the first crack was observed in leeward side column at ground storey at 14th cycle against 30.03 kN. The amount of displacement in A1 frame was found increased almost linearly and seems the displacement was smooth and stable, see Fig. 13(a). The frame A1 almost lost their strength at 60.04 kN within 24 cycles corresponding displacement 60 mm. Similarly, the displacement of first and ground floor at 14th cycle was 8 and 5 mm respectively, see Fig. 13(b)-(c). At failure, the displacement at second, first and ground floor was 60, 32 and 22 mm respectively.

The hysteresis response of A16 frame was measured at ground, first and second floor level against cyclic loading is shown in Fig. 14(a)-(c). First crack was observed as interface bonding crack at ground and first floor at 8th cycle against 16.4 kN, however the first crack was observed in beam column joint at ground and first storey on 11th cycle against 22.18 kN with displacement of 8 mm. The frame A16 almost lost their strength at 40 kN within 21 cycles corresponding displacement 65 mm. Similarly, the displacement of first and ground floor at 11th cycle was 4.1 and 3.6 mm respectively, see Fig. 13(b)-(c). The maximum displacement on second, first and ground floor was 47, 39 and 22.8 mm respectively was observed on 20th cycle i.e. before last cycle. However at failure, the displacement on second, first and ground floor was 65, 34 and 19 mm respectively was observed on 21st cycle and the yielding was seen clearly in Fig. 15. The peak load corresponding displacement of the frames A0, A1 and A16 was measured from Figs. 12-14 at first quarter (x, y) is shown in Fig. 15. It is concluded that the behaviour of A16 is highly preferable since the amount of displacement is less and insignificant damage on infill as well as frame, Fig. 11(c). In principle, failure mechanism of an infilled frame depends to a great extent on the relative strength of the frame and the infill, Mehrabi *et al*. (1996).

The storey drift of frame during first crack and onset of failure has been compared and discussed in this section. The storey drift of bare frame, infilled frame at first, second and third storey has been measured is shown in Fig. 16(a)-(c). At first crack, the behaviour of A0 and A16 in all three storey level was found same and the displacement is

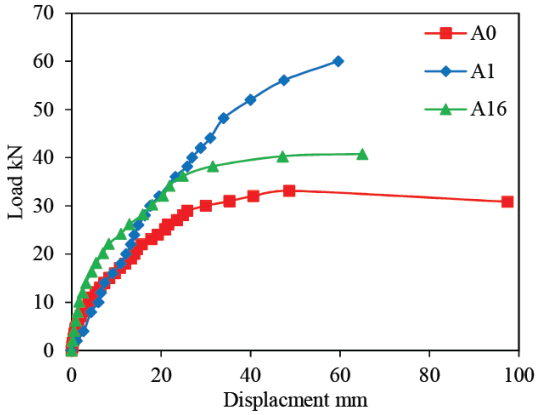

Fig. 15 Second storey lateral displacement of frames at peak point of x and y quarter

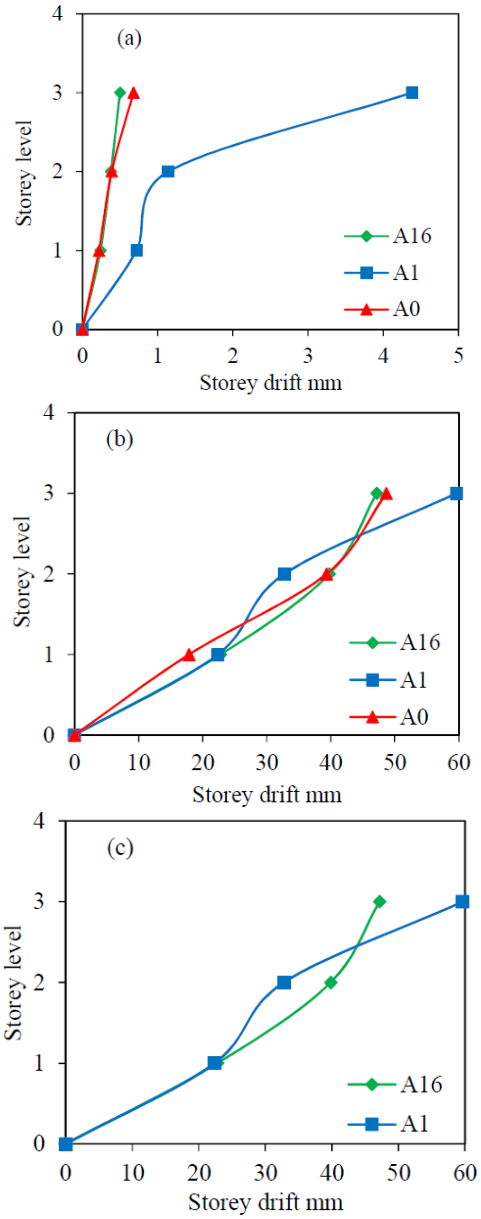

Fig. 16 Lateral displacement of frames at (a) before crack and comparison of onset of final crack of (b) A0, A1 and A16 and (c) A1 and A16 frame

insignificant, less than 1 mm. However the displacement on second storey of A1 frame was 4.38 mm, whereas at first and ground storey was almost 1 mm, Fig. 16(a). At failure of A1 frame, the storey drift was found as 60, 32 and 22 mm at second, first and ground floor respectively. Onset of failure, the storey drift on A0 and A16 frame was found almost same, see Fig. 16(b). It is concluded that the presence of interface materials such as foam on first floor of A16, the drift was increased (39.3 mm) as compare to frame A1 (32.78 mm). However the efficiency due to use of cork and foam on A16 frame at ground and first storey the drift at second storey was reduced significantly, Fig. 16(c).

The deflection ductility factor is defined as Δ/Δ_y, where Δ and Δ_y is deflection at any load beyond yield and deflection 5.34, 15.77 and 8.35 mm at yield load of the frame A0, A1 and A16, respectively. The frame A0 has

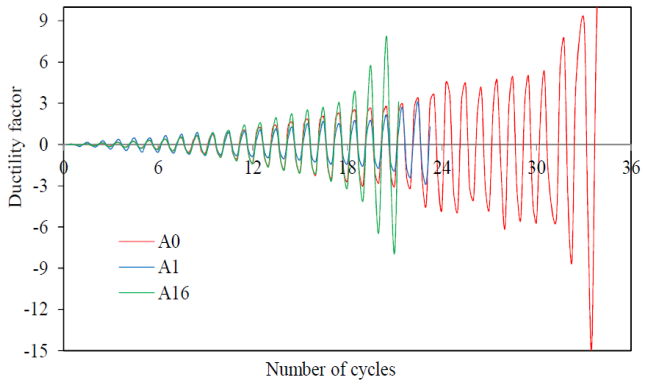

Fig. 17 Ductility factor function of number of cycles

maximum ductility factor equal to 14.8 whereas frames A16 has 7.8 and A1 has only 2.8, see Fig. 17. This signifies provision of various interface materials on A16 frame increases ductility factor by (7.8-2.8/2.8)*100=160%. The ductility factor of A16 frame was found decreased by (14.75-7.84/14.75)*100=47% as compare to A0 frame. However the ductility factor of A1 frame was found decreased by (14.75-2.83/14.75)*100=81% as compare to A0 frame. Therefore, it is concluded that overall efficiency of A16 frame was found increased by (81-47/81)*100= 42% as compare to A1 frame. From the Fig. 17, it's clear that the number of cycles to failure for A0, A16 frame is more when compare to A1 frame. This also signifies that the ductility of A16 frame is more than the A1 frame due to the increased stiffness of A1 frame.

5. Comparison of experimental and non-linear finite element analysis

The non-linear finite element analysis has been carried out to estimate the strength capacity of a structure beyond its limit state to its ultimate strength. The results thus obtained through numerical simulations in terms of first crack load, ultimate load, location of plastic hinges, crack pattern on infill and stress on infill has been compared with the experiments and discussed in this section.

5.1 Non-linear analysis

The static Non-linear analysis was performed of bare frame as well as infilled frame using SAP2000. The two-bay three-storey frame members were modelled as beam and column line elements, while the infill and interface elements were modelled as shell elements with plane sections and discussed in Section 2.3. The hinge properties for column and beams were assigned as per FEMA356 are already available in SAP. The behaviour has been predicted by assigning deformation controlled hinge type is called ductile hinges that describes effective strengths of material, FEMA356. For both column and beam P-M2-M3 type hinge were assigned in the present study. The moment rotation curve of a P-M2-M3 hinge is a monotonic backbone relationship used to describe the post-yield behaviour of a beam-column element subjected to

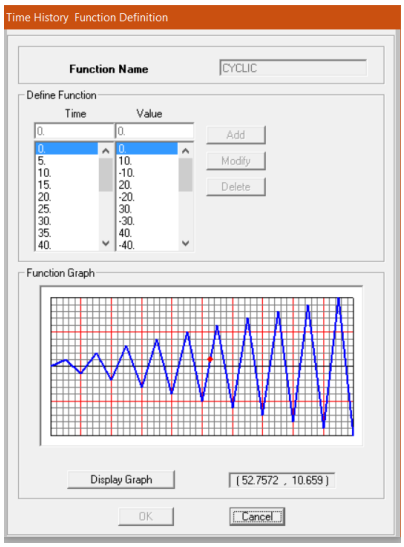

Fig. 20 Description of loading function on module of SAP programme

combined axial and biaxial-bending conditions, SAP 2000.

5.2 Time history analysis

Time history analysis has been carried out for given bare frame as well as infilled frames against static cyclic loading. The loading function in terms of time versus amplitude was defined as the cyclic loading with 1 kN as increment achieved by each cycle as shown in Fig. 20. The loading function was defined is same used to carryout experiments, refer Fig. 10. The response of bare frame as well as infilled frame has been predicted. The results thus obtained through numerical simulations in terms of first crack load, ultimate load, location of plastic hinges, crack pattern on infill and stress on infill has been compared with the experiments and discussed in the upcoming section.

5.3 Comparison of experimental and numerical results

Experimental and numerical studies has been carried out to investigate the performance of integral infill reinforced concrete frames under in-plane lateral loading. In this Section, the numerical results are concisely summarized and findings are compared with the experiments. The initial crack load, ultimate load, location of plastic hinges, crack pattern on infill and stresses has been predicted using time history analysis has been compared with the experiments and summarized below.

The initial crack load was predicted using SAP is compared with the experimental results is shown in Table 5. In general, the predicted initial crack load and experiments was found reasonably in good agreement. The deviation on overall predicted initial crack load was found insignificant when compare to experimental results. However, the predicted results through simulations are under estimated for all three frames. The ultimate load was predicted and compared with the experimental results are shown in Table 6. For A0 and A1 frame, the predicted results and

Table 5 Comparison of initial crack load

Frame designation	Experimental results kN	Numerical results kN	Maximum deviation (%)	Remarks
A0	12.05	10.50	13	Under estimated
A1	30.03	26.50	12	Under estimated
A16	22.18	19.00	14	Under estimated

Table 6 Comparison of ultimate load

Frame designation	Experimental results kN	Numerical results kN	Maximum deviation (%)	Remarks
A0	33.15	30.5	8	Under estimated
A1	60.04	64.5	7	Over estimated
A16	40.32	36.2	15	Under estimated

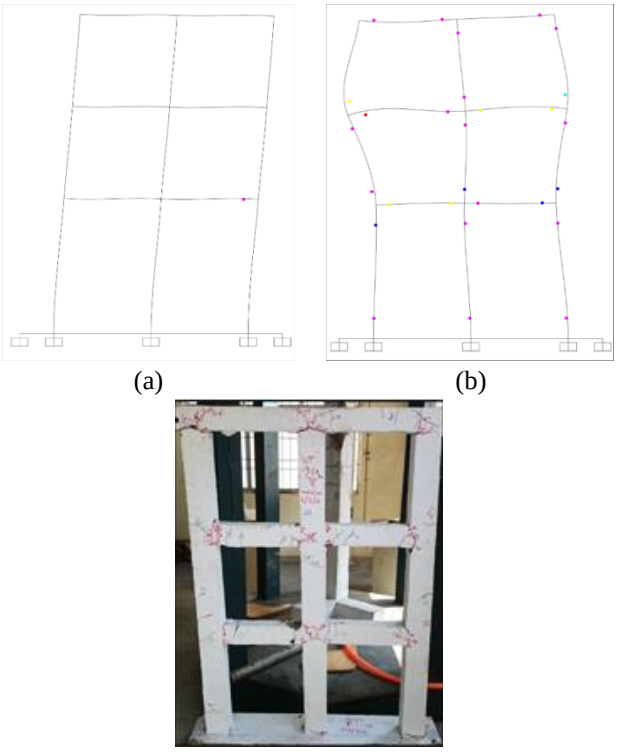

Fig. 22 Deformed profile of bare frame with (a) initial hinge (b) finial hinge predicted numerically compared with (c) the experiment

experiments was found reasonably in good agreement. The predicted results of bare frame through simulations are under predicted whereas the results of infilled frame A16 under predicted.

The actual and predicted failure mechanism of bare frame was compared in Fig. 22(a)-(c) and a close correlation between the two has been found. Initial crack was observed in the leeward (pull) side of the beam column joint of bare frame during experiment and same crack was predicted in simulations, Fig. 22(a). The failure of A0 frames was predicted numerically at 30.5 kN corresponding

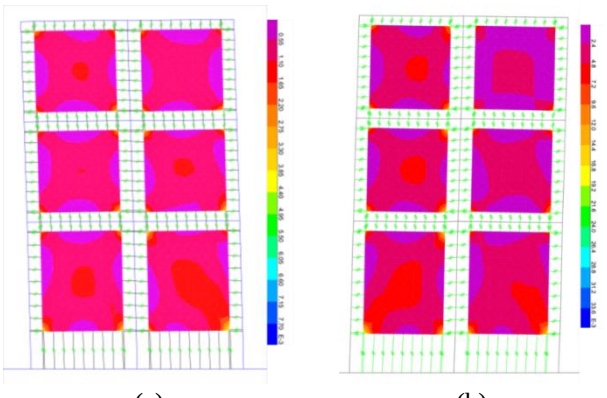

(a) (b)

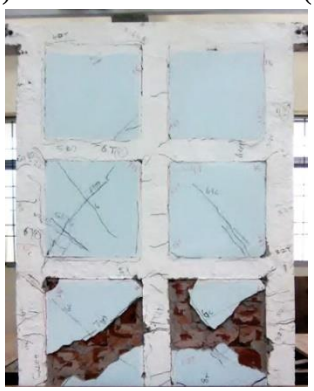

(c)

Fig. 23 Deformed profile of A1 frame with (a) initial hinge stage (b) finial hinge stage predicted numerically compared with (c) the experiment

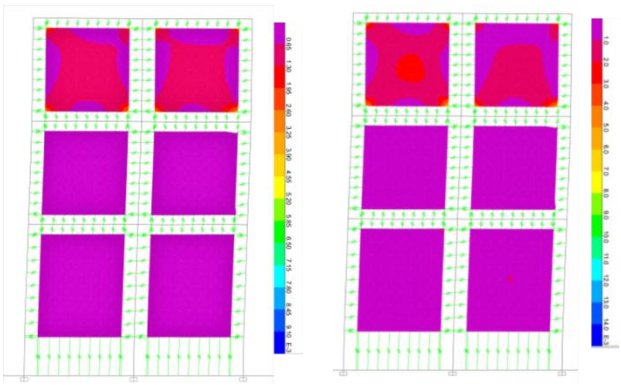

(a) (b)

(c)

Fig. 24 Deformed profile of A16 frame with (a) initial hinge stage (b) finial hinge stage predicted numerically compared with (c) the experiment

hinges are shown in Fig. 22(b) whereas it has been observed experimentally at 32.6 kN corresponding deformed profile is shown in Fig. 22(c). The pink and yellow colour indicates the hinges at yielding and failure of the structures, refer Section 5.1. An exact pattern of deformation as in the form of hinges (yellow colour) has been predicted through the finite element simulations at first floor level on beam and it is confirmed through experiments. Overall, the simulations predicted the critical hinges at first and second floor level of bare frame was found closely matching and it is clearly visible in the experimental results.

The actual and predicted failure mechanism of infilled frame A1 was compared in Fig. 23(a)-(c) and a close correlation between the two has been found. The damage was indicated in the infill in terms of von-Mises stresses and it is presented in "kN/mm^2". First crack was observed in leeward side column at ground storey against 30.03 kN during experiment and it is predicted through numerical simulations the stress concentration at ground storey of leeward side column, see Fig. 23(a). An exact pattern of deformation on infill wall has been predicted through the finite element simulations for all given panel. The chipping of material at the infill surface although could not be reproduced however, higher stresses developed in that region describe the proximity with the actual findings, Fig. 23(b). The pattern of stresses predicted in the infill is in closest agreement with that of the observed chipping at ground storey, Fig. 23(c).

The predicted failure mechanism of infilled frame A16 was compared with the experiment, see Fig. 24(a)-(c). In general, the simulations predicted the deformation in masonry infill however, The maximum von-Mises stress on infill was predicted as 9.1 and 14 MPa during 16.4 and 36.2 kN respectively, see Fig. 24(a)-(b). It should be noted that experimentally the first crack was observed as interface de-bonding at ground and first floor at 16.4 kN and the first crack was observed in beam column joint at ground and first floor at 22.18 kN. However, the simulations predicted no stress concentration on ground and first floor infill, but in second floor corners of infill influenced by maximum von-Mises stress, see Fig. 24(b). There is no diagonal crack in the infill was predicted as well as measured on both ground and first floor. Also, it is observed that several small cracks for all the elements of ground and first storey, except for the frame members at second storey, Fig. 24(c).

6. Conclusions

The nonlinear behaviour of integral infilled frames (in which the infill and the frame are bonded together) is studied both experimentally and numerically. The effect of various interface materials such as cement mortar, cork and foam on the performance of infilled frame has been studied and following conclusions are drawn.

Linear finite element analysis has been carried out to

quantify the effect of combination of various interface materials on the infilled frames. Studies were conducted on 21 modified infilled frame cases. It is concluded that the configuration with three interface materials offered better resistance among the chosen modified frames and hence, the experiments were performed on bare frame, conventional infilled frame with cement mortar interface and modified infilled frame with different interface materials.

The behaviour of bare frame as well as infilled frames was studied in terms of the initial cracking and ultimate load, hysteresis behaviour of frame, storey drift and ductility ratio.

The failure of conventional infilled frame occurred at 60 kN, almost twice that of the bare frame (33.15 kN). It may be concluded that the infill panels significantly enhance both the stiffness and strength of the frame.

In case of modified infilled frame, failure occurred at 40 kN and the resistance was decreased by 30% as compared to conventional infilled frame; but compared to bare frame, it increased by 20%. Also no diagonal crack in infill wall was observed at the ground and first storey of modified frame whereas in case of conventional frame the chipping of material and wide crack at the infill surface were observed.

When foam was used as the interface material on first floor of modified infilled frame, the drift increased (39.3 mm) compared to conventional frame (32.78 mm). The combination of cork and foam on the modified frame at ground and first storey increased the drift at the second storey by 16%. Therefore, it is concluded that the behaviour of modified frame is highly preferable since the amount of displacement is high and no significant damage occurs on infill as well as frame.

The ductility ratio of modified infilled frame increased by 42% when compared to the conventional infilled frame and decreased by 47% as compared to bare frame. This also signifies that the ductility of modified infilled frame is more than that of the conventional infilled frame. This may be due to the increased stiffness of rigid interface infilled frame.

The difference in ultimate load between the experimental and numerical results was only 7-15%, suggesting that the numerical studies were in accordance with reality.

The predicted failure mechanisms and predicted stress concentration of infill influenced by maximum von-mises stress were similar to those observed during experiments.

References

Al-Chaar, G., Issa, M. and Sweeney, S. (2002), "Behavior of masonry infilled non-ductile reinforced concrete frames", *J. Struct. Eng*., ASCE, **128**, 1055-1063.

Anil, O. and Altin, S. (2007), "An experimental study on reinforced concrete partially infilled frames", *Eng. Struct.*, **29**, 449-460.

Asteris, P.G. (2003), "Lateral stiffness of brick masonry infilled plane frames", *J. Struct. Eng*., ASCE, **129**(8), 1071-1079.

Buonopane, S.G. and White, R.N. (1999), "Pseudodynamic testing of masonry-infilled reinforced concrete frame", *J. Struct. Eng*., **125**(6), 578-589.

CSI (2000), Integrated Software for Structural Analysis and Design: Analysis Reference Manual, Computer and Structures, Berkeley, CA.

Dhanasekar, M. and Page, A.W. (1986), "Influence of brick masonry infill properties on the behavior of infilled frames", *Proc., Instn. Civil Eng*., **81**(2), 593-605.

Dogangun, A., Ural, A. and Livaoglu, R. (2008), "Seismic performance of masonry buildings during recent earthquakes in turkey", *Proceedings of the 14th World Conference on Earthquake Engineering*, Beijing, China, October.

Erdik, M. and Aydinoglu, N. (2003), "Earthquake vulnerability of buildings in Turkey", *Proceedings of the 3rd International Symposium on Integrated Disaster Risk Management*, Japan, July.

FEMA 356 (2000), Prestandard and commentary for the seismic rehabilitation of buildings, Federal Emergency Management Agency; Washington, DC, USA.

Ghosh, A.K. and Amde, A.M. (2002), "Finite element analysis of infilled frames", *J. Struct. Eng.*, ASCE, **128**(7), 881-889.

Ibrahimbegovic, A. (1990), "A Novel membrane finite element with an enhanced displacement interpolation", *J. Finite Elem. Anal. Des.*, **7**, 167-179.

IS 10262 (2009), Concrete mix proportioning - Guidelines, Bureau of Indian Standards, New Delhi.

IS 13920 (1993), Ductile detailing of reinforced concrete structures subjected to seismic forces - Code of practice, Bureau of Indian Standards, New Delhi.

IS 456 (2000), Plain and Reinforced Concrete - Code of Practice, Bureau of Indian Standards, New Delhi.

Key, D. (1988), *Earthquake Design Practices for Buildings*, Thomas Telford Ltd., Telford House, London.

Khoshnoud, H.R. and Marsono, K. (2016), "Experimental study of masonry infill reinforced concrete frames with and without corner openings", *Struct. Eng. Mech*., **57**(4), 641-656.

Klingner, R.E. and Bertero, V.V. (1978), "Earthquake resistance of infilled frames", *J. Struct. Div.*, ASCE, **104**(ST6), 973-87.

Liauw, T.C. and Kwan, K.H. (1984), "Nonlinear behaviour of non-integral infilled frames", *Comput. Struct.*, **18**, 551- 560.

Mallick, D.V. and Garg, R.P. (1971), "Effect of openings on the lateral stiffness of infilled frames", *Proc., Instn. Civil Eng*., **49**, 193-209.

Mallick, D.V. and Severn, R.T. (1967), "The behaviour of infilled frames under static loading", *Proc., Instn. Civil Eng*., **38**, 639-656.

Mehrabi, A.B., Shing, P.B., Schuller, M. and Noland, J. (1996), "Experimental evaluation of masonry-infilled RC frames", *J. Struct. Eng.*, **122**(3), 228-237.

Moghaddam, H.A. (2004), "Lateral load behavior of masonry infilled steel frames with repair and retrofit", *J. Struct. Eng*., ASCE, **130**(1), 56-63.

Muthukumar, S., Joson Western, J. and Satyanarayanan, K.S. (2017), "Analytical study on nonlinear performance of RC two bay three storeyed frames with infill", *Asian J. Civil Eng.*, **18**(1), 133-149.

Riddington, J.R. (1984), "The influence of initial gaps on infilled frame behavior", *Proc. Inst. Civil Eng., Part 2*, **77**, 295-310.

Satyanarayanan, K.S. (2009), "Studies on the influences of different materials on the elastic behaviour of infilled frames", A Thesis of Doctor of Philosophy at SRM University, Chennai.

Satyanarayanan, K.S. and Lakshmipathy, M. (2009), "Conceptualisation studies on the development of adaptive interface in infilled frames", *Int. J. Appl. Eng. Res.*, **4**(1), 1579-1589.

Senthil, K. (2010) "Influence of interface thickness and pattern on the behavior of in-filled frames", A Dissertation of Master of

Technology at SRM University, Chennai.
Senthil, K. and Satyanarayanan, K.S. (2016), "Influence of interface on the behavior of infilled frame subjected to lateral load using linear analysis", *Coupl. Syst. Mech.*, **5**(2), 127-144.
Senthil, K., Satyanarayanan, K.S. and Rupali, S. (2016), "Behavior of fibrous reinforced concrete systems subjected to monotonic and cyclic loading", *The 10th Structural Engineering Convention, CSIR-SERC*, IIT Madras, Chennai, India, December.
Senthil, K., Satyanarayanan, K.S. and Rupali, S. (2016), "Energy absorption of fibrous self-compacting reinforced concrete system", *Adv. Concrete Constr.*, **4**(1), 37-47.
Smith, B.S. (1966), "Behavior of square infilled frames", *J. Struct. Div.*, ASCE, **ST1**, 381-403.

CC